

The Heat Budget of the TOGA-COARE Domain in an Ocean Model

PETER R. GENT

National Center for Atmospheric Research, Boulder, Colorado

The annual mean heat budget of the TOGA-COARE domain is examined in a reduced-gravity, primitive equation model of the upper equatorial ocean that is described by Gent and Cane (1989). It is forced by the monthly winds from Rasmusson and Carpenter (1982), and the heat flux formulation is from Seager et al. (1988). It is concluded that the annual mean net heating of the ocean surface in the area 140°E - 180°E, 10°S - 10°N is between 0 and 20 W m⁻². This is considerably less than the estimates given in climatic atlases which vary from about 30 W m⁻² (Esbensen and Kushnir, 1981; Hsiung, 1985), about 50 W m⁻² (Weare et al., 1981), to about 70 W m⁻² (Reed, 1985). These estimates have no physical constraints on the analysis, whereas the model result is constrained by the ocean's ability to remove heat from the TOGA-COARE domain.

1. INTRODUCTION

The Coupled Ocean-Atmosphere Response Experiment of the Tropical Ocean-Global Atmosphere program (TOGA-COARE) was proposed for the area 140°E - 180°E, 10°S - 10°N in the western tropical Pacific. This area has one of the highest sea surface temperatures (SSTs) found anywhere and is an area where the mean winds are light. Thus the relative importance of thermodynamic to wind stress forcing of the ocean is probably higher in this area than most other places in the world's oceans.

Estimates of the annual mean net heating of the ocean surface in climatic atlases vary from about 30 W m⁻² [Esbensen and Kushnir, 1981; Hsiung, 1985] to about 50 W m⁻² [Weare et al., 1981] to about 70 W m⁻² [Reed, 1985]. However, evidence is increasing that the annual mean net heating is considerably smaller than these estimates. The evidence comes both from direct observations in the TOGA-COARE area [Godfrey and Lindstrom, 1989] and from numerical models [Gordon, 1988; Seager et al., 1988].

In this paper, the annual mean heat budget of the TOGA-COARE domain is examined in a new reduced-gravity, primitive equation model of the upper equatorial ocean. The model has been designed for El Niño-Southern Oscillation (ENSO) studies. Thus there is particular emphasis on thermodynamic processes because sea surface temperature is the most important ocean variable to the atmosphere. The model domain is limited in both the horizontal and vertical; thus this primitive equation model uses the reduced-gravity assumption so that the deep ocean is at rest below the active upper ocean. This assumes that only the near equatorial upper ocean is important for the dynamic and thermodynamic processes of the TOGA problem on the time scale of a few years. The model is described in detail by Gent and Cane [1989]; therefore section 2 contains only a brief description of the model and the forcing. The heat flux parameterization is described by Seager et al. [1988], and its unique feature is that it does not depend upon air temperature or humidity. Seager et al. [1988, p. 1269] state,

Copyright 1991 by the American Geophysical Union.

Paper number 90JC01677.
0148-0227/91/90JC-01677\$05.00

The thesis here is that air temperature is determined by the SST, not the other way around. To include it in a heat flux parameterization is to include a constraint on the SST tantamount to putting in a large part of the answer.

The heat budget of the TOGA-COARE domain in the basic model run plus 4 variants is described in section 3. Section 4 is a discussion, and the conclusion is that the annual mean net heating of the ocean surface in the TOGA-COARE area is between 0 and 20 W m⁻².

2. THE MODEL AND FORCING

The reduced-gravity model is described in detail by Gent and Cane [1989]. Only the essential details and recent model additions will be discussed here. The model equations use a generalized vertical coordinate, s , and in this coordinate frame are

$$h = \frac{\partial z}{\partial s} \quad (1)$$

$$\frac{\partial P}{\partial s} = hb \quad (2)$$

$$b = \alpha g(T - T_B) \quad (3)$$

$$\frac{\partial}{\partial t}(h\mathbf{u}) + \nabla \cdot (\mathbf{u}h\mathbf{u}) + \frac{\partial}{\partial s}(w_e\mathbf{u}) + \mathbf{f} \times h\mathbf{u} + h(\nabla P - b\nabla z) = \tau + \frac{\partial}{\partial s}\left(\frac{\nu_v}{h}\frac{\partial \mathbf{u}}{\partial s}\right) \quad (4)$$

$$\frac{\partial}{\partial t}(hT) + \nabla \cdot (\mathbf{u}hT) + \frac{\partial}{\partial s}(w_eT) = Q + \frac{\partial}{\partial s}\left(\frac{\kappa_v}{h}\frac{\partial T}{\partial s}\right) \quad (5)$$

$$\frac{\partial h}{\partial t} + \nabla \cdot (h\mathbf{u}) + \frac{\partial w_e}{\partial s} = 0 \quad (6)$$

T_B is the fixed temperature of the deep ocean taken to be 10°C and $\alpha g = 2.5 \times 10^{-3} \text{ m s}^{-2} \text{ C}^{-1}$. P represents the dynamically active part of the pressure and is zero at the model base, consistent with the reduced-gravity approximation which assumes there is no motion in the deep ocean. Angle brackets denote a horizontal average, and the generalized vertical velocity is, by definition,

$$w_e = h \frac{Ds}{Dt} \quad (7)$$

The vertical coordinate, s , is defined by making a choice for w_e and this choice can be different in various parts of the model domain. For simplicity the depth of the mixed layer, where the forcing acts, is kept constant at 50 m by applying the condition that

$$w_e \text{ (base of ML)} = \nabla \cdot (h\mathbf{u})(\text{ML}) \quad (8)$$

Thus in the mixed layer h is a constant, s is just a scaled depth, and w_e is the usual vertical velocity. At the model base w_e is taken to be zero and the temperature is fixed at T_B . Since the model does not have a dynamically active salinity, the model base is an isopycnal surface. Thus the model base is a function of x , y , and t and is calculated from (6); its average value is constant and is taken to be 400 m. The depth between the base of the mixed layer and the model base is divided up into 6 model layers that are fixed, prescribed fractions of this depth. Thus, between the base of the mixed layer and the model base, s is a sigma coordinate and w_e , which is not the usual vertical velocity, is calculated appropriately. The first 5 of these layers have an average depth of 50 m and the lowest layer has an average depth of 100 m. The ocean domain is rectangular covering the area from 130°E to 80°W and from 30°S to 30°N. The resolution is uniform of 1° in longitude and is stretched smoothly in latitude increasing from 0.25° at the equator to 1° at 30°N and 30°S. Nonlinear computational instability in the model is controlled by use of a Shapiro filter which is of order 16 in the interior reducing to order 2 at the boundaries.

Richardson number-dependent vertical mixing has been added to the model since the description given by *Gent and Cane* [1989]. The Richardson number, Ri , is calculated at model interfaces, so that it represents a bulk Ri over 50 m. The vertical eddy diffusivity and conductivity are given by

$$\begin{aligned} \nu_v &= 10^3 / (1 + 10Ri)^2 + \nu_B(s) \text{ cm}^2 \text{ s}^{-1} \\ \kappa_v &= 10^3 / (1 + 10Ri)^3 + \kappa_B(s) \text{ cm}^2 \text{ s}^{-1} \end{aligned} \quad (9)$$

The background values ν_B, κ_B are functions of depth and, over the area between 21°N and 21°S, ν_B varies between 1 and 2 $\text{cm}^2 \text{ s}^{-1}$ and κ_B varies between 0.5 and 1 $\text{cm}^2 \text{ s}^{-1}$. Between 21°N and 21°S and the meridional boundaries, ν_B and κ_B increase linearly to values 10 and 2 times the values quoted above, respectively. In these regions the currents are weak and the Richardson number mixing is seldom used. The first functional form in (9) was chosen to go from the large value of $10^3 \text{ cm}^2 \text{ s}^{-1}$ when $Ri = 0$ to match the background value when $Ri \approx 3$. In fact, if the Ri in a column is greater than 3 everywhere, then only the background mixing is implemented. The second form in (9) has the same value of $10^3 \text{ cm}^2 \text{ s}^{-1}$ when $Ri = 0$, but decreases more quickly to match the background value when $Ri \approx 1.2$. The forms (9) are smoothed versions of the observations of *Peters et al.* [1988]. The smoothing is appropriate because the numerical model is discretized over layers about 50 m deep, whereas the vertical scale of the observations is about 6 m. The background values in (9) are larger than in the observations (see the discussion in section 3.4).

The winds used to force the model are the monthly climatological winds of *Rasmusson and Carpenter* [1982]. The actual winds used are linear interpolations of these values between the midpoints of the months. The wind stress was calculated by

$$\boldsymbol{\tau} = \rho_a C_D \mathbf{u} | \mathbf{u} | \quad (10)$$

where $10^3 \rho_a = 1.2 \text{ g cm}^{-3}$ and $10^3 C_D = 1.67$, a high value which can be justified by the fact that monthly mean winds are being used.

The heat flux parameterization is that of *Seager et al.* [1988] with the coefficients given by the best fit analysis of *Blumenthal and Cane* [1989]. Thus

$$\begin{aligned} Q &= (1 - A)(1 - 0.76C + 0.0019\theta)Q_0 \\ &- \rho_a C_{EL} | \mathbf{u} | (1 - \delta)q(\text{SST}) - \alpha(\text{SST} - T^*) \end{aligned} \quad (11)$$

The incoming solar flux depends upon the albedo ($A = 0.06$); the cloud cover, C (taken from *Esbensen and Kushnir* [1981] as the annual average fraction of cloud cover); the solar altitude, θ ; and the clear sky flux, Q_0 . The latent heat flux depends upon the wind speed (which has a minimum value of 4 m s^{-1} because the mean wind speed is underestimated by the speed of the mean wind when it is small), the saturation humidity evaluated at the sea surface temperature $q(\text{SST})$, and δ (0.78). Here $\delta q(\text{SST})$ equals q (atmospheric temperature) times the relative humidity. This formulation was chosen so as to be a function of SST alone and not to be dependent upon a fixed atmospheric temperature. This gives the ocean model SST more freedom to change significantly than if an atmospheric temperature is used to specify Q . The sum of the sensible and longwave heat flux, which is the smallest term in the tropics, is simply parameterized with $\alpha = 1.8 \text{ W m}^{-2} \text{ C}^{-1}$ and $T^* = -2.78^\circ \text{C}$.

3. RESULTS

3.1. Basic Case

The model was integrated from rest and run for 16 years, at which time it had attained a statistical equilibrium. This was determined by the fact that the interannual changes in model total energy and heat content integrated over the domain were less than 2% of the seasonal changes in these quantities.

The annual average temperature along the equator down to 400 m is shown in Figure 1. The simulation is quite realistic in the western Pacific with an SST of between 29°C and 30°C and a relatively deep warm pool with a temperature of 25°C at 150 m. Between 150 and 260 m is the sharp equatorial thermocline with the temperature at 260 m being 14°C. The simulation in the eastern Pacific is not so realistic because the thermocline is more diffuse than in reality. SSTs of 23°C to 24°C, however, are realistic for this region. The annual average SST between 20°S and 20°N is shown in Figure 2. As just mentioned, the SST at the equator is quite realistic, but SSTs off the equator are generally too warm. This is especially true in the southern hemisphere in the central Pacific south of 5°S. This illustrates the sensitivity of the simulated SST field to the model forcing. The parameters used in the heat flux formulation (11) were based on a best fit to observed Pacific SSTs in a much simpler ocean model using the winds

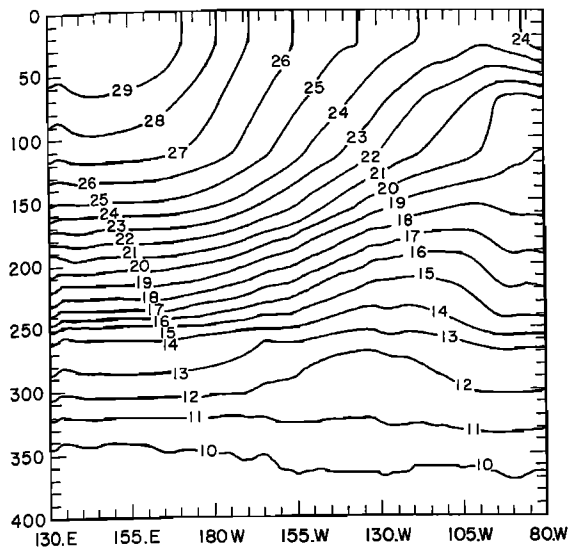


Fig. 1. The annual average temperature along the equator from 130°E–80°W down to 400 m in the basic case. Contour interval is 1°C.

produced at Florida State University (FSU) [Blumenthal and Cane, 1989]. The Rasmusson and Carpenter winds are considerably weaker than the FSU winds in this area of the Pacific which results in a smaller evaporative heat loss term in (11). Thus the SST increases until it is large enough so that the other terms can balance the incoming solar radiation in (11). This accounts for the SST of 32°C in the southern, subtropical Pacific. This also shows that the coefficients in (11) are dependent on the winds used and are probably also somewhat dependent on the ocean model used.

The annual mean net heat flux into the ocean between 20°S and 20°N is shown in Figure 3. Along the equator values range from about 10 W m⁻² in the west to 80 W m⁻² in the east and do not vary much during the year. Away from the equator the net heat flux varies considerably during the year, but the annual mean values vary between

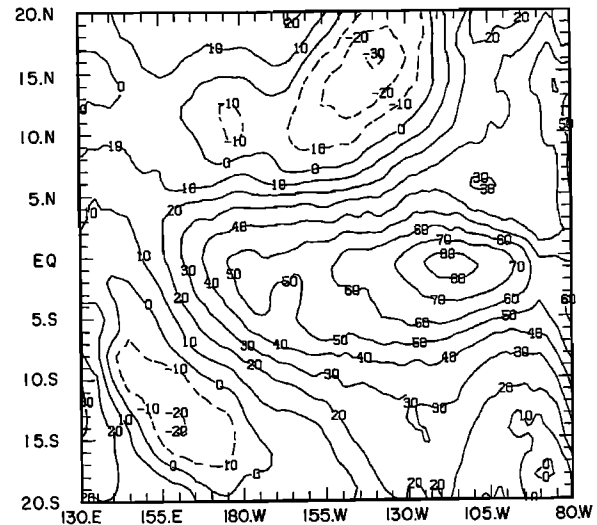


Fig. 3. The annual mean net heat flux into the ocean between 130°E–80°W, and 20°S–20°N in the basic case. Contour interval is 10 W m⁻².

about -30 and 30 W m⁻² in the two subtropical regions. Figure 3 shows that the annual mean net heat flux in the TOGA-COARE region varies considerably ranging from 50 W m⁻² into the ocean on the equator near the dateline to 10 W m⁻² into the ocean on the equator near 140°E to 10 W m⁻² into the atmosphere near 180°E, 10°N and 150°E, 10°S. Figure 4 shows the annual average SST between 20°S and 20°N such that the annual mean net heat flux into the ocean is zero. This is determined by turning off all the dynamics and diffusion in the model and setting the depth of the upper mixed layer to 1 m. The model quickly converges to a state of no motion with a residual heat flux of less than 2 W m⁻². Comparison of Figures 2 and 4 shows, especially on the equator, the relative importance of dynamics and thermodynamics in determining SST. In the western equatorial Pacific the two SSTs are almost the same so that the SST is determined primarily by

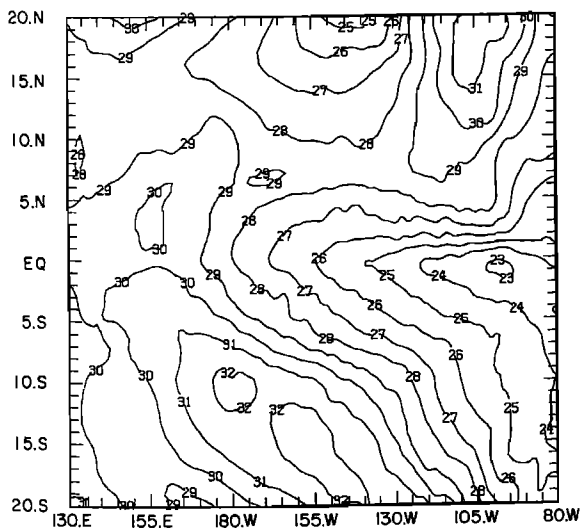


Fig. 2. The annual average SST between 130°E–80°W, and 20°S–20°N in the basic case, Contour interval is 1°C.

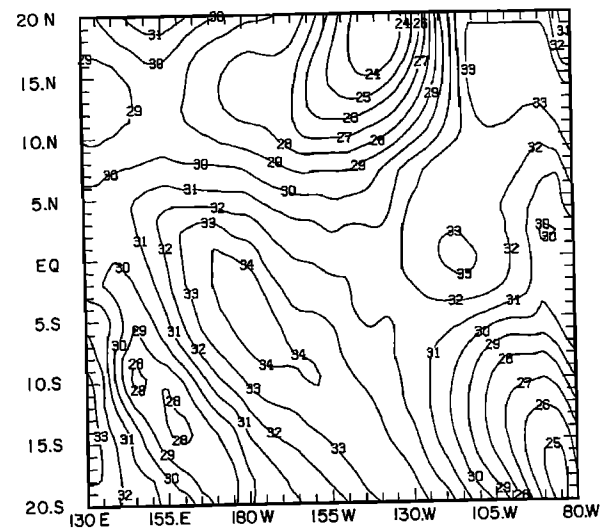


Fig. 4. The annual average SST between 130°E–80°W, and 20°S–20°N such that $Q = 0$ in the basic case. Contour interval is 1°C.

ocean thermodynamics; whereas, in the eastern equatorial Pacific the two SSTs are 10°C different so that the SST is determined primarily by ocean dynamics.

The heat budget of the TOGA-COARE domain has been analyzed in the model. The heat budget over $140^{\circ}\text{E} - 180^{\circ}\text{E}$, $10^{\circ}\text{S} - 10^{\circ}\text{N}$ and 0 to 50 m (i.e., upper layer only) over the annual cycle of the sixteenth year of model integration is

$$\begin{aligned} \frac{\partial}{\partial t}(hT) = & \text{-Advection} + \text{Heat Flux} \\ & -3.9 \quad 13.5 \\ & \text{-Vertical Diffusion} \\ & -9.0 \text{ W m}^{-2} \end{aligned} \quad (12)$$

The residual of 0.6 W m^{-2} is balanced to some extent by small terms due to the Richardson number mixing and horizontal filtering in the model. The remainder of the residual arises because the values of hT at the start and end of the model year are not the same, so that the time rate of change term on the left-hand side of (12) is small, not zero. The heat flux and advection break down into components as follows:

$$\begin{aligned} \text{Heat Flux} = & \text{Incoming Solar} - \text{Latent} \\ 13.5 & \quad 189.8 \quad -117.6 \\ & \text{-(Sensible + Longwave)} \\ & -58.7 \text{ W m}^{-2} \end{aligned} \quad (13)$$

$$\begin{aligned} \nabla \cdot (h\mathbf{u}T) = & \frac{\partial}{\partial x}(huT) + \frac{\partial}{\partial y}(hvT) \\ 3.9 & \quad -157.2 \quad 175.8 \\ & + \frac{\partial}{\partial s}(w_e T) \\ & -14.7 \text{ W m}^{-2} \end{aligned} \quad (14)$$

The three-dimensional divergence from (6) was also calculated in the volume over the year as was the average SST, which is 29.86°C . Thus the three-dimensional advection can also be broken down as

$$\begin{aligned} h\mathbf{u} \cdot \nabla T = & hu \frac{\partial T}{\partial x} + hv \frac{\partial T}{\partial y} + w_e \frac{\partial T}{\partial s} \\ 3.9 & \quad 6.8 \quad -4.1 \quad 1.2 \text{ W m}^{-2} \end{aligned} \quad (15)$$

This shows that, on average, there is upwelling into the mixed layer, since w_e is positive. This is balanced by meridional flow out of the volume, which tends to heat the volume, and zonal flow, which tends to cool the volume. However, all of these heat advections are very small both because the currents in the TOGA-COARE mixed layer are small and the temperature gradients are weak. Thus advection cannot remove much heat and neither can vertical diffusion because the vertical temperature gradient is weak and there is little mixing. The result is that the annual mean net heat flux into the ocean is quite small; the model value averaged over the TOGA-COARE area is 13.5 W m^{-2} . The incoming solar radiation is mostly balanced by latent and sensible plus longwave heat loss, and these two components are in the ratio of 2:1.

The annual cycles of the incoming solar flux, outgoing latent flux, and net heat flux into the TOGA-COARE area are shown in Figure 5. The net heat flux has a dominant semiannual signal from the solar flux that is modified by a smaller annual signal from the latent heat flux. The annual cycle of the ocean response is shown in Figure 6. The average SST shows a dominant semiannual signal that gives a corresponding signal in the heat storage term defined to

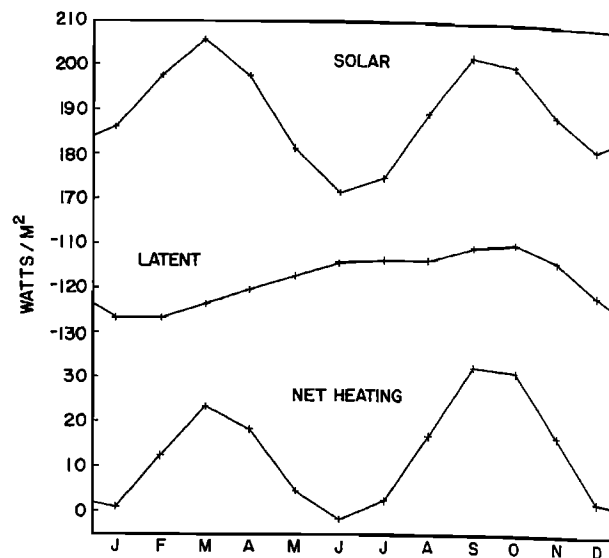


Fig. 5. The annual cycle of incoming solar flux, outgoing latent flux, and net heat flux Q given by (12) averaged over the TOGA-COARE area.

be $h\rho C_p d(SST)/dt$, where SST are the monthly averages shown in Figure 6a and h is 50 m, the depth of the upper layer. Subtracting the heat storage from the net heat flux gives the annual cycle in the advection plus diffusion term, which is shown in Figure 6c. It is clear from Figures 5 and 6 that thermodynamically controlled quantities, which include SST, show a dominant semiannual signal, whereas dynamically controlled quantities show a dominant annual signal. This is to be expected since the dynamics are dominated by wind forcing and *Trenberth et al.* [1990] show that, in the TOGA-COARE area, the annual variation dominates and accounts for more than 60% of the variance in both components of the wind stress.

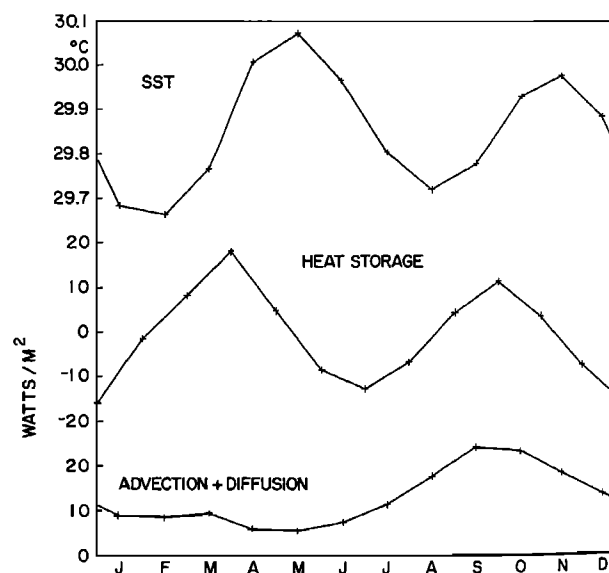


Fig. 6. The annual cycle of SST, heat storage, and advection plus diffusion averaged over the upper 50 m in the TOGA-COARE domain.

3.2. Minimum Wind Speed of 3 m s^{-1}

In order to test the robustness of the small net heating, 4 other cases were run. In the first the minimum wind speed threshold in the latent heat flux term in (11) was reduced from 4 to 3 m s^{-1} . The model was then run for 4 more years which meant it was again almost in statistical equilibrium. The heat budget in the TOGA-COARE area over the upper 50 m in the last year is

$$\begin{aligned} \frac{\partial}{\partial t}(hT) = & \text{-Advection} + \text{Heat Flux} \\ & -4.0 \quad 17.7 \\ & \text{- Vertical Diffusion} \\ & - 13.3 \text{ W m}^{-2} \end{aligned} \quad (16)$$

The SST at the end of this model run is shown in Figure 7. The temperature in the TOGA-COARE area has risen because of the initial reduced latent heat flux loss. The SST rises until heat loss due to latent and sensible plus longwave again almost balances the solar heating. The annual mean net heating of the ocean in this case is 17.7 W m^{-2} . The ocean SSTs produced in this run, shown in Figure 7, are unrealistically high and the average SST in the TOGA-COARE area is 31.56°C . In the minimum wind speed 4 m s^{-1} run, the latent heat flux was also calculated if the minimum was 3 m s^{-1} . The result is that the annual mean latent heat loss calculated like this is 100.1 W m^{-2} . Thus reducing the minimum wind speed to 3 m s^{-1} is equivalent to an additional mean net heat flux of 17.5 W m^{-2} which resulted in an increase of average SST of 1.7°C . Thus the sensitivity of the TOGA-COARE area to increases in net heat flux is very strong in this ocean model. In fact

$$\text{Sensitivity} = \frac{dT_s}{dQ} = 0.1^\circ\text{C m}^2 \text{ W}^{-1} \quad (17)$$

i.e., it only takes a 10 W m^{-2} change in heat flux to induce a 1°C change in model SST. This value is slightly larger than that of Seager *et al.* [1988], which is about $0.08^\circ\text{C m}^2 \text{ W}^{-1}$ in the TOGA-COARE area, and indicates that the

more comprehensive model used in this study is somewhat more sensitive than the simpler model used by Seager *et al.* [1988].

3.3. No Ri Mixing, Larger ν_B, κ_B

The version of the model described by Gent and Cane [1989] has no Richardson number mixing term, and the vertical diffusion is solely due to the eddy diffusivity and conductivity ν_B and κ_B . With no Richardson number mixing, larger values of ν_B and κ_B are needed to keep the solution stable; in particular, to keep a positive vertical temperature gradient everywhere in the domain. This model run has values of ν_B and κ_B 10 and 2 times larger than in the basic case, respectively. Thus ν_B and κ_B are functions of s varying between 10 and $20 \text{ cm}^2 \text{ s}^{-1}$ and 1 and $2 \text{ cm}^2 \text{ s}^{-1}$, respectively. The coefficients of eddy diffusivity and conductivity in this case are larger than those considered valid for the upper tropical ocean.

The annual average temperature along the equator down to 400 m for this case is shown in Figure 8. The SST in the western Pacific on the equator is between 28°C and 29°C and comparison with Figure 1 shows that this is about 1°C cooler than in the basic case. Also in this case with larger ν_B and κ_B , the western Pacific thermocline is not as sharp and, hence, the warm pool is not as deep as in the basic case, which has smaller ν_B and κ_B and Richardson number mixing. A heat budget analysis over the TOGA-COARE domain down to 50 m has been performed over an annual cycle, and the result is

$$\begin{aligned} \frac{\partial}{\partial t}(hT) = & \text{-Advection} + \text{Heat Flux} \\ & -4.9 \quad 24.0 \\ & \text{-Vertical Diffusion} \\ & -18.7 \text{ W m}^{-2} \end{aligned} \quad (18)$$

In this case the vertical diffusion term is more than twice that in the basic case and the advection is again very small. These two terms balance the annual mean heat flux which, in this case, is 24 W m^{-2} .

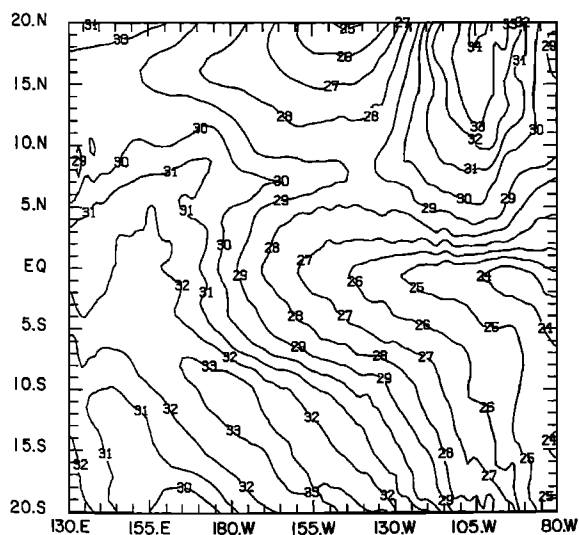


Fig. 7. The annual average SST between 130°E – 80°W and 20°S – 20°N in the case when the minimum wind speed in the latent heat term in (11) is 3, not 4 m s^{-1} . Contour interval is 1°C .

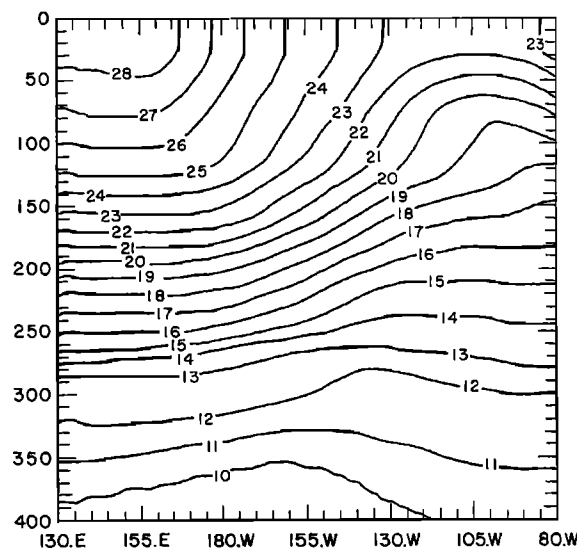


Fig. 8. The annual average temperature along the equator between 130°E – 80°W down to 400 m in the case with no Ri mixing and larger values of ν_B and κ_B . Contour interval is 1°C .

3.4. Smaller κ_B

Another run was performed which differed from the basic case only in the fact that κ_B was reduced by a factor of 5 between 21°N and 21°S. Thus this case has Ri mixing and ν_B and κ_B vary between 1 and 2 cm² s⁻¹ and 0.1 and 0.2 cm² s⁻¹, respectively. From their observations *Peters et al.* [1988] calculate $\nu_B = 0.2$ cm² s⁻¹, $\kappa_B = 0.01$ cm² s⁻¹ which are still an order of magnitude smaller than the values used in this case.

The annual mean net heat flux into the ocean between 20°S and 20°N is shown in Figure 9. Comparison with Figure 3 shows little difference in pattern, but the magnitude of the mean flux is uniformly about 10 W m⁻² less than in the basic case. Thus the annual mean net heat flux into the TOGA-COARE area has been reduced by about 10 W m⁻². The heat budget of the TOGA-COARE area over the upper 50 m in the last year of this case is

$$\begin{aligned} \frac{\partial}{\partial t}(hT) = & \text{-Advection} + \text{Heat Flux} \\ & -2.1 \quad 3.5 \\ & \text{-Vertical Diffusion} \\ & -1.9 \text{ W m}^{-2} \end{aligned} \quad (19)$$

Compared to the basic case, the vertical diffusion is reduced by almost a factor of 5, which is to be expected since the vertical temperature gradient remains almost unchanged. Thus with smaller κ_B , the annual mean net heat flux into the TOGA-COARE area is very small and is 3.5 W m⁻².

3.5. FSU Winds

The model was also run using the monthly climatological winds produced at Florida State University. These were determined by averaging over the monthly wind products from 1961 to 1987. These winds are considerably stronger than the *Rasmusson and Carpenter* [1982] winds so that a reduced drag coefficient of $10^3 C_D = 1.25$ is more appropriate than the higher value used before. This case has Ri mixing and the small values of ν_B and κ_B given in section 3.4.

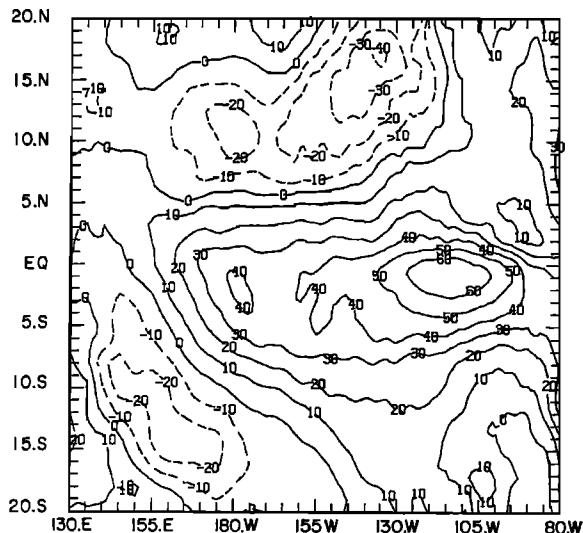


Fig. 9. The annual mean net heat flux into the ocean between 130°E–80°W and 20°S–20°N in the case with the smaller value of κ_B . Contour interval is 10 W m⁻².

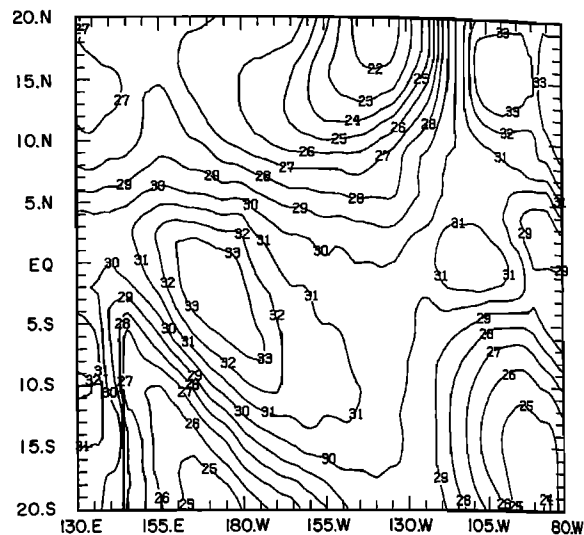


Fig. 10. The annual average SST between 130°E–80°W and 20°S–20°N such that $Q = 0$ in the case using FSU winds. Contour interval is 1°C.

Figure 10 shows the annual average SST between 20°S and 20°N such that the annual mean net heat flux into the ocean is zero using the FSU winds. Comparison with Figure 4 shows that the values in this case are smaller everywhere because the FSU winds are considerably stronger than the *Rasmusson and Carpenter* winds. The differences are mostly about 2°C or less, except east of Northern Australia where they reach 4°C in a very small area. The heat budget of the TOGA-COARE area over the upper 50 m in the last year of integration is

$$\begin{aligned} \frac{\partial}{\partial t}(hT) = & \text{-Advection} + \text{Heat Flux} \\ & -3.4 \quad 6.6 \\ & \text{-Vertical Diffusion} \\ & -2.8 \text{ W m}^{-2} \end{aligned} \quad (20)$$

Compared to the case in section 3.4, this budget shows that the advection and diffusion are somewhat stronger using the FSU winds so that the heat flux needed to balance them is larger. Using the FSU winds the annual mean net heat flux into the TOGA-COARE area is 6.6 W m⁻².

4. DISCUSSION AND CONCLUSIONS

All the cases presented in section 3, except that in section 3.3, have an annual mean net heat flux into the ocean in the TOGA-COARE region of less than 20 W m⁻². The value for the case in section 3.3 is 24 W m⁻², most of which is balanced by vertical diffusion. Cases in sections 3.3, 3.4, and 3.5 show that the size of the vertical diffusion term is almost directly proportional to κ_B and the value of κ_B in section 3.3 is larger than that considered valid for the upper tropical ocean. The three-dimensional advective heat flux is very small in all cases because of weak currents and very weak temperature gradients. The Richardson number mixing flux is very small in all cases because the Ri criterion of less than 3 for mixing is seldom satisfied because of weak velocity shears in the TOGA-COARE region of the model.

Section 3.2 shows that if the net heat flux is made larger, for example by setting a smaller minimum wind speed in the latent heat flux term, then the upper ocean just heats up until a new balance is reached where the net heat flux is again less than 20 W m^{-2} . The opposite would be true if the mean net heat flux was somehow reduced. Note that the latent heat flux could be changed by different values of C_E or δ in (11) as well as by changing the minimum wind speed, and that the net flux could have been changed by varying the other flux components. All would have given the same result. This shows that the SSTs in this area are mostly determined by ocean thermodynamics rather than by dynamics. The SST in the TOGA-COARE area is very sensitive to changes in the heat flux with a change of 10 W m^{-2} giving rise to a change of 1°C in SST. This explains why ocean models used with the much larger heat flux estimates from atlases have very high SSTs in the western Pacific and also means that confidence limits on the net heat flux calculated from this ocean model are quite small. In fact, the conclusion from this work is that, with a high degree of confidence, the annual mean net heat flux into the ocean in the TOGA-COARE area is between 0 and 20 W m^{-2} .

After reaching this conclusion, the author was referred to a recent paper by Gordon [1988, p. 266], which describes results from a coupled model of the United Kingdom Meteorological Office climate model and a high resolution version of the GFDL model. Gordon says,

...further uncoupled experiments with the ocean model have indicated that 20 W m^{-2} is an upper limit to the surface heat flux if the model is to reproduce the observed SSTs. Essentially, there is no mechanism which can remove heat from the mixed layer at a rate high enough to balance a large heat input.

This is in complete agreement with the present study. Other models of the annual cycle in the tropical Pacific Ocean have been run by Schopf and by Philander *et al.* [1987]. Both models use somewhat different heat flux parameterizations and have values of the annual mean net heat flux into the ocean on the equator slightly larger than that shown in Figure 3. Both studies also have annual mean heat flux out of the ocean off the equator in the TOGA-COARE area, so that their average values for the TOGA-COARE area would be slightly higher than in the present model.

There is observational evidence to support the conclusions of this model study. Enfield [1986] estimates horizontal advection and diffusion from data and finds values less than 20 W m^{-2} between 150°E and 180°E . In fact, the advection estimate is zero between 150°E and 160°E . In addition, Niiler and Stevenson [1982] estimate vertical diffusion from observations in the western Pacific. They estimate the diffusion across isotherms rather than across particular depths. The diffusion across the 28°C and 26°C isotherms is $5\text{--}19 \text{ W m}^{-2}$ and $5\text{--}17 \text{ W m}^{-2}$, respectively. All of these observational estimates are quite small, and the model estimates given in (12) are not inconsistent with these observational estimates. There is also some recent evidence from direct heat flux measurements in the TOGA-COARE area that the mean net heat flux is less than 20 W m^{-2} . Godfrey and Lindstrom [1989] report

observations over a period of 2 weeks generally during light winds and deduced a net heat flux of 10 W m^{-2} or less into the ocean. These estimates from direct observations are much smaller than those of the climatologies in the TOGA-COARE area, e.g., 30 W m^{-2} [Esbensen and Kushnir, 1981; Hsiung, 1985], 50 W m^{-2} [Weare *et al.*, 1981], and 70 W m^{-2} in [Reed, 1985]. It should be noted that these estimates are not subject to the physical constraints that are present in the numerical model.

There are at least 4 possibilities for these overestimates.

(1) The cloud cover and the cloud coefficient of 0.62 in (11) are underestimated giving too much incoming solar radiation. (2) The mean wind speed is underestimated by the speed of the mean wind, so that the latent flux is underestimated. Clearly the minimum wind speed value of 4 m s^{-1} is an ad hoc fix for this problem. (3) The latent heat flux is underestimated in light winds by the usual flux formula. (4) The sensible heat flux is underestimated because the average air-sea temperature difference used was too small.

REFERENCES

- Blumenthal, M. B., and M. A. Cane, Accounting for parameter uncertainties in model verification: An illustration with tropical sea surface temperature, *J. Phys. Oceanogr.*, **19**, 815–830, 1989.
- Enfield, D. B., Zonal and seasonal variations of the near-surface heat balance of the equatorial Pacific Ocean, *J. Phys. Oceanogr.*, **16**, 1038–1054, 1986.
- Esbensen, S. K., and Y. Kushnir, The heat budget of the global ocean: An atlas based on estimates from surface marine observations, *Climate Res. Inst. Rep.*, **29**, 27pp., Oregon State Univ., Eugene, 1981.
- Gent, P. R., and M. A. Cane, A reduced gravity, primitive equation model of the upper equatorial ocean, *J. Comput. Phys.*, **81**, 444–480, 1989.
- Godfrey, J. S., and E. Lindstrom, On the heat budget of the equatorial West Pacific surface mixed layer, *J. Geophys. Res.*, **94**, 8007–8017, 1989.
- Gordon, C., A study of air-sea interactions in the tropical Pacific with a coupled GCM, Modelling the Sensitivity and Variations of the Ocean-Atmosphere System, WCRP-15, pp. 262–270, World Clim. Res. Prog., Geneva, Switzerland, 1988.
- Hsiung, J., Estimates of global meridional heat transport, *J. Phys. Oceanogr.*, **15**, 1405–1413, 1985.
- Niiler, P. P., and J. Stevenson, The heat budget of tropical ocean warm-water pools, *J. Mar. Res.*, **40** (Suppl.), 465–480, 1982.
- Peters, H., M. C. Gregg, and J. M. Toole, On the parameterization of equatorial turbulence, *J. Geophys. Res.*, **93**, 1199–1218, 1988.
- Philander, S. G. H., W. J. Hurlin, and A. D. Seigel, Simulation of the seasonal cycle of the Tropical Pacific Ocean, *J. Phys. Oceanogr.*, **17**, 1986–2002, 1987.
- Rasmusson, E. M., and T. H. Carpenter, Variations in tropical sea surface temperature and surface wind fields associated with the Southern Oscillation/El Niño, *Mon. Weather Rev.*, **110**, 354–384, 1982.
- Reed, R. K., An estimate of the climatological heat fluxes over the tropical Pacific Ocean, *J. Climate Appl. Meteorol.*, **24**, 833–840, 1985.

Seager, R., S. E. Zebiak, and M. A. Cane, A model of the tropical Pacific sea surface temperature climatology, *J. Geophys. Res.*, *93*, 1265–1280, 1988.

Trenberth, K. E., W. G. Large, and J. G. Olson, The mean annual cycle in global ocean wind stress, *J. Phys. Oceanogr.*, *20*, 1742–1760, 1990.

Weare, B. C., P. T. Strub, and M. D. Samuel, Annual mean surface heat fluxes in the tropical Pacific Ocean, *J. Phys. Oceanogr.*, *11*, 705–717, 1981.

P. R. Gent, National Center for Atmospheric Research, P. O. Box 3000, Boulder, CO 80307.

(Received November 16, 1989;
revised April 16, 1990;
accepted May 4, 1990.)